A bypass circuit for avoiding the hot spot in PV modules

Guerriero, Pierluigi; Tricoli, Pietro; Daliento, Santolo

Link to publication on Research at Birmingham portal

A Bypass Circuit for Avoiding the Hot Spot in PV Modules

Pierluigi Guerriero[1], Pietro Tricoli[2], Santolo Daliento[1*]

[1] Department of Electrical Engineering and Information Technology, University of Naples Federico II,
80125 Naples, Italy
[2] School of Electronic, Electrical and Systems Engineering, University of Birmingham
Edgbaston, Birmingham, B15 2TT, UK
*corresponding author: daliento@unina.it

Abstract

The hot spot occurring in outlier solar cells is recognized as one of the main reliability issues for photovoltaic modules. Even though PV modules are qualified to sustain over-temperatures the hot spot can lead to accelerated aging and, sometimes, to unexpected failure; in severe cases, with the possible risk of fire. The standard countermeasure to contrast this phenomenon is the adoption of bypass diodes, whose role is to limit the maximum reverse voltage across outlier cells. However, since the current is not limited, power dissipation can be high. In this paper a bypass circuit,suited to completely avoiding the onset of the hot spot, is presented. The circuit is a substantial improvement of a previous version that was able to reduce power dissipation by reducing the voltage across the reverse biased solar cell. The improvement presented in this paper allow to completely cancel the current, thus avoiding power dissipation and, therefore, preventing the rising in temperature of the solar cell. The novelty with respect to comparable approaches is that the intervention of the circuit doesn't require the preliminary detection of the hot spot. Indeed, the circuit self-activates in the same operating conditions of standard diodes, without needing neither control logic nor power supply. Detailed circuit simulations and experiments are presented to evidence the capability of the circuit to fully prevent power dissipation, and consequent rising in temperature, in outlier cells.

Keywords: hot spot, bypass diode, reliability, PV systems.

I.   Introduction

In the last years the Photovoltaic (PV) technology experienced a huge increase of the installed capacity. In many countries the achievement of the fuel parity pushed large investments in the construction of new photovoltaic plants, as witnessed by the increment of tens of Gigawatt installed worldwide last year(Philipps and Warmuth, 2018). Among other factors, one of the key points which favored the success of this technology is its modularity, which makes the construction of utility scale power stations almost as easy as small scale domestic plants, with very reduced time to market. However, this strength is the major

weakness of the PV technology as well; in fact, the modularity means that thousands of elements (photovoltaic modules, which are in turn made of tens of series connected solar cells (Green, 1986)), are hardwired to build the desired power size. The consequence is that both fault location and fault fixing are extremely challenging and time-consuming issues. By taking in mind that the Return Of Investment (ROI), is not only dependent on the expected lifetime of the power plant, but also on the continuity of the power production, it is clear that plant shutdown for maintenance interventions should be avoided or, at least, minimized. It is quite obvious that the best strategy to prevent production losses, and consequent maintenance queries, is to improve the reliability of photovoltaic modules. In this regard, it is widely recognized that one of the main issues (Jordan and Kurtz, 2013; Kaplani, 2012; Sanchez-Friera et al., 2011)affecting the probability of faults in photovoltaic modules is the formation of hot spots (García et al., 2013), that is over-temperature typically localized on a portion of a solar cell. It should be remarked that the occurrence of hot spots is absolutely usual during normal operation of PV fields; indeed, the rising in temperature can be triggered by the simple presence of partial shading, even of very small area, like that caused by leaves or birth drops. In such conditions, in fact, solar cells get reverse biased, thus dissipating power and getting hot. In order to limit the maximum reverse bias, photovoltaic modules are equipped with bypass diodes that, as well explained in (Green, 1986), automatically turns on in presence of current mismatches. Unfortunately, bypass diodes cannot avoid the hot spot (Kim and Krein, 2015)occurrence. This fact means that photovoltaic modules should be manufactured to sustain over-temperatures without damages. In principle, the ability to sustain hot spots is certified for each model of commercially available photovoltaic module, by the qualification procedure dictated by the EN 61215 rules. This procedure verifies that the power dissipated by the hot spot cell, depending on the correct sizing of the bypass diode ("AN3432 ST Application note," 2011), is low enough to avoid failures. However, it has been evidenced (Kim and Krein, 2015) that, due to the spread of solar cell parameters, damages can occur even though operating conditions are within expected safe limits. Moreover, it should be considered that recurring hot spot events can lead to accelerated ageing (Olalla et al., 2018), thus increasing the fault probability.

Above arguments lead to the conclusion that the over-temperature should be limited as much as possible. As mentioned above the main protecting strategy involves the adoption of bypass diodes. Indeed, as it is widely known, almost all crystalline photovoltaic modules are equipped with such diodes. Even though, as clarified in (Kim and Krein, 2015), they cannot avoid the hot spot, but just limit power dissipation, they have the fundamental feature to be fully compatible with the normal operation of photovoltaic modules, by automatically activating themselves only when, because of some current mismatch, the voltage supplied by the photovoltaic module reverses. Actually, whether or not the bypass diode, in case of mismatch, turns ON, is largely due the control algorithms for the Maximum Power Point Tracking

71 (MPPT). These algorithms can decide to lower the overall current delivered by the PV system, thus

72 avoiding the turning ON of the bypass diode and the consequent reverse biasing of the outlier solar cell.

73 Thus, a strategy which is encountering some success for limiting the hot spot, is based on the ability to

74 recognize its occurrence so as to instruct the MPPT to keep the operating point of the system in a safe

75 region (Spanoche et al., 2013). For example, in (Bressan et al., 2018) a shadow emulator based on FPGA

76 is exploited to foresee the possible occurrence of hot spot. The limit of this approach is that it does not

77 work for unexpected shadows coming from rubbish covering the cell; moreover, in such approaches, the

78 power delivered by the whole system is dramatically reduced, because the current is limited to that

79 supplied by the worst performing solar cell.

80 Different strategies presented so far involve improved bypass circuits able to reduce (or even suppress) the

81 power dissipated in the reverse biased solar cell (D'Alessandro et al., 2014; Ghanbari, 2017; Niazi et al.,

82 2018).

83 In this regard, it should be noted that power dissipation can be totally avoided by forcing the current to

84 zero. Such a feature can be achieved by inserting a series switch for breaking the circuit when the

85 conditions for the triggering of the hot spot are recognized, as for example proposed in (Dhimish et al.,

86 2018). In such a case the key point is the reliable detection of unsafe operating conditions. In (Dhimish et

87 al., 2018) thermal images were exploited to directly identify hot cells; after that, a series connected power

88 MOSFET was driven in the OFF state. A more effective detection system was presented in (Kim et al.,

89 2013), where the change of impedance of the monitored PV string is assumed as a sign of the presence of

90 the hot spot. The detection required to periodically interrupt the MPPT to acquire the I-V curve of the

91 string. When the hot spot is detected the current is interrupted by means of a series MOSFET. The

92 drawback of this approach is that requires a microprocessor for each photovoltaic module; moreover, its

93 effectiveness depends on the frequency of the I-V scan, in other words, the hot spot is not prevented, it is

94 just suppressed some amount of time after its appearing.

95 In order to overcome the above drawback and with the aim to combine the benefits of the series switch

96 with the self-activation of the standard bypass diode, a modified bypass circuit was presented in (Daliento

97 et al., 2016). It exploited the decreasing voltage across the shaded photovoltaic module to drive in the

98 pinch-off operating region a series connected MOSFET. As a result, the reverse voltage appearing across

99 the shaded solar cell was diminished by the drain to source voltage of the MOSFET, thus transferring

100 dissipated power from the solar cell to the power MOSFET. By adopting that circuit, the temperature of

101 the hot cell decreased of some tens of Celsius degree; however, over-temperature was not completely

102 avoided and the warming of the junction box (where the MOSFET was hosted) was a critical issue.

103   In this paper a substantial improvement of the circuit proposed in (Daliento et al., 2016) is presented.

104   Differently from the previous solution, the new bypass circuit is able to completely suppress the current

105   flowing into the reverse biased solar cell. Therefore, power dissipation cannot occur and the rising in

106   temperature is fully prevented. As a result, the onset of the hot spot is totally avoided. Moreover, since the

107   current is cancelled, the power MOSFET doesn't dissipate power and the warming of the junction box is

108   prevented as well.

109   The new circuit still exploits the voltage across the photovoltaic module to drive the series connected

110   power MOSFET, thus guaranteeing self-activation. The difference with respect to (Daliento et al., 2016)is

111   a special designed driving circuit (see Fig.3), allowing the complete switching OFF of the series

112   MOSFET.As will be shown in the following sections, the behavior of a photovoltaic module equipped

113   with the proposed circuit is, from the terminals point of view, almost identical to that of a photovoltaic

114   module equipped with a standard bypass diode.

115   The paper is organized as follows. Section II introduces the new circuit in comparison with the previous

116   one. Section III provides a detailed description of the polarization and gives information about realization

117   costs. Section IV describes actual operating modes achieved by means of circuit simulations. Section V

118   reports experimental results. Finally, conclusions are drawn in Section VI.

119

120   **II. Bypass circuit operating principle**

121

122   As mentioned above the circuit proposed in this paper is an evolution of the circuit presented in (Daliento

123   et al., 2016). In order to point out differences and new functionalities the previous circuit is shown in Fig.

124   1b, while the additions proposed in this paper are shown in Fig. 2 and Fig. 3.Only the main features of this

125   topology will be recalled here, more details can be found in (Daliento et al., 2016).
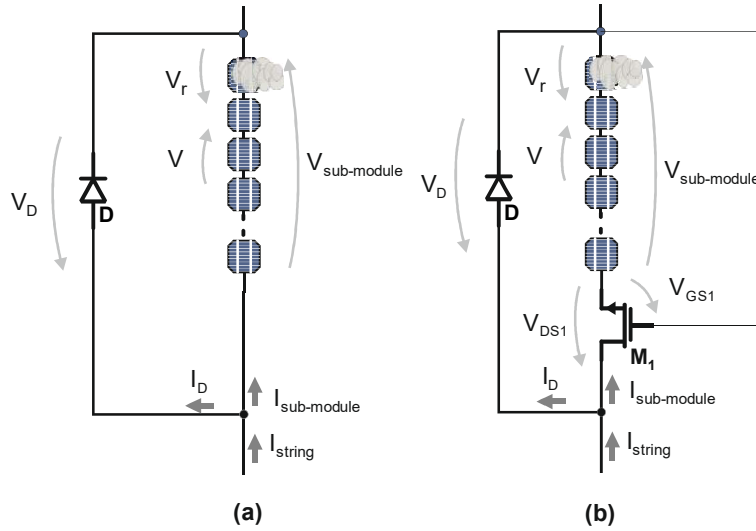
126

Fig. 1. Series of solar cells protected by standard bypass diode
(a) and by an improved bypass circuit subtracting part of the
reverse voltage from the shaded cell (b).

As can be seen, the figure shows both the standard arrangement (Fig. 1a), with a bypass diode "protecting" a group of N series connected solar cells (hereinafter referred to as sub-module), and the modified circuit (Fig. 1b), with the MOSFET M_1 connected in series with the sub-module. The most important detail to note is that M_1 is directly driven by the voltage, $V_{sub\text{-}module}$, supplied by the sub-module, which coincides with V_{GS1}. During normal operation (uniform irradiation and no limiting cells) this voltage is positive and quite high (about 10 V since the bypass diode is usually parallel connected to the series of about 20 solar cells). This voltage is high enough to push M_1 in deep conduction where it exhibits a residual resistance of just few milliohms. In other terms, during uniform irradiation the presence of M_1 is negligible and does not affect the behavior of the photovoltaic module. Conversely, when a solar cell limits the current supplied by the module (as an example because it is shadowed), the excess of current coming from the string deviates through the bypass diode, which limits to V_D the voltage at its terminal. Therefore, the reverse voltage across the limiting cell is

$$V_r = (N-1)V + V_D, \tag{1}$$

in the standard case of Fig. 1a, while it is

$$V_r = (N-1)V + V_D - V_{DS1}, \tag{2}$$

in the presence of M_1.

In (2) (as shown in (Daliento et al., 2016)) V_{DS} weakly depends on the current mismatch, being at least equal to the threshold voltage of M_1.

150   The drawback of the circuit of Fig. 1b is that M_1 gets hot in place of the shaded cell.

151   In order to overcome this issue, the circuit shown in Fig. 2 could be adopted.

152   Two operating modes can be identified. The first corresponds to uniform behavior of all solar cells. In

153   such a case the circuit operation is identical to that of Fig. 1b. Indeed, M_1 operates in deep conductions, so

154   that V_{DS1} is low. As can be seen, V_{DS1} is the driving voltage for M_2 (coincides with the gate-source voltage

155   of M_2), thus M_2 is kept OFF and has no effects on the circuit. The second operating mode occurs in case of

156   current mismatch between I_{string} and $I_{sub-module}$. In such a case a positive feedback activates; indeed, V_{DS1}

157   increases (as in the circuit of Fig. 1b) thus turning ON the MOSFET M_2, with the consequence that V_{DS2}

158   decreases. Since V_{DS2} coincides with V_{GS1}, M_1 is driven in the OFF state and the current through the sub-

159   module is completely interrupted (while the string current, I_{string}, flows through the bypass diode).

160
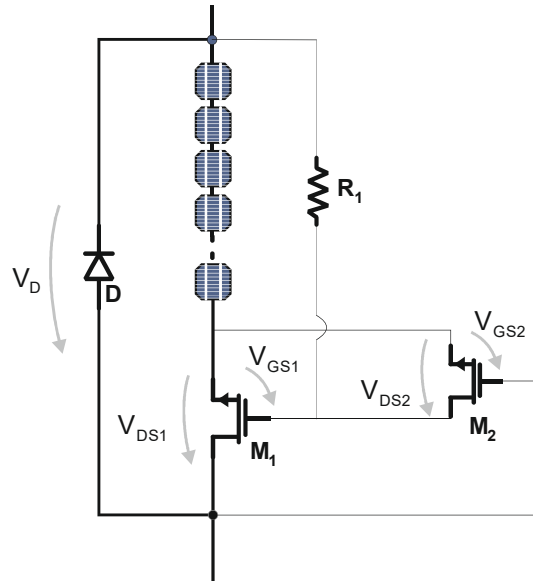

161

162   Fig. 2. Improved bypass circuit with a feedback MOSFET M_2
163   to switch off the sub-module current.

164

165   Unfortunately, this very simple solution does not work well because the conduction of M_1 can not be

166   recovered when the current mismatch ceases. In fact, once M_1 has been interdicted, the rising of the

167   current is always prevented, even though the conditions for the bypass are removed.

168   Therefore, the circuit which is actually proposed in this paper is that of Fig. 3.

169   As can be seen, the feedback MOSFET M_2 is now driven by the output voltage of a digital oscillator

170   TLC555. The oscillator is power supplied by V_{DS1}. Hence, as long as V_{DS1} is low (normal operation) the

171   oscillator is switched OFF, its output is low and M_2 is OFF as well. When bypass conditions occur, V_{DS1}

172   increases, the oscillator turns ON and starts to provide output signals alternatively high and low. As will

173   be shown in the next sections the duty cycle of the oscillator is chosen in such a way that the output signal

174   is kept high for about 97% of the time. During this interval of time M_2 is ON and, as a consequence, M_1 is

175   kept OFF. The lowering of the output signal of the oscillator can be seen as an attempt to turn ON M_1, if

176   bypass conditions are still present when the output of the oscillator returns to high V_{DS1} returns high as

177   well and, for another 97% of the time, the current cannot flow. Conversely, if bypass conditions are no

178   longer present, the attempt to turn ON M_1 succeeds, V_{DS1} falls down, and the oscillator gets switched OFF,

179   thus returning in the normal operating conditions.

180
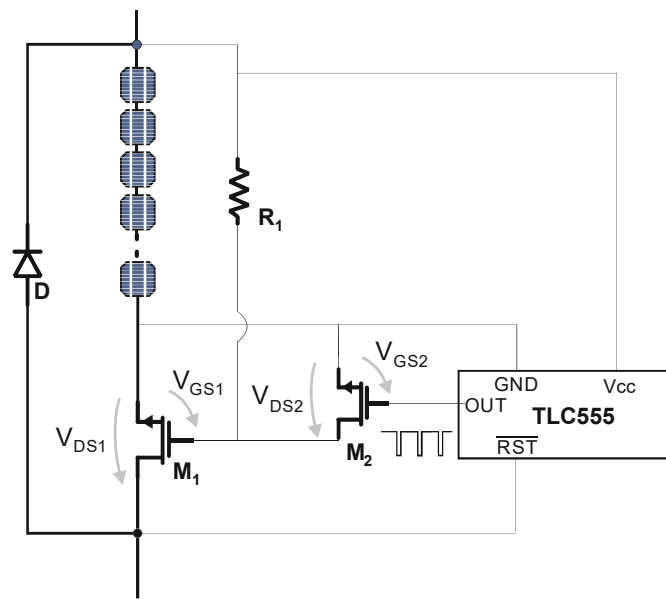
181

182   Fig. 3. New bypass circuit for the prevention of the hot spot.

183

184   The above solution fully prevents the rising in temperature of shaded cells. Moreover, differently from

185   other approaches, the circuit does not exploit microprocessors or other logic components. It is also

186   important to note that the circuit only consumes a negligible amount of power during bypass events, since

187   the TLC555 is sleeping for the rest of the time.

188   It is useful to note that the operation of the bypass circuit is strictly related to the architecture of the solar

189   module. The present form was designed for monocrystalline and polycrystalline solar modules, which are

190   made by groups (sub-modules) of series connected solar cells with accessible terminals. The proposed

191   circuit is not suitable for thin film technologies, because those solar panels are made by monolithically

192   integrated solar cells that do not give access to the internal terminals.

193 However, it is worth to point out that thin film solar panel based on multijunction solar cells can be

194 designed in such a way that each solar cell is provided with its own monolithically integrated bypass

195 diode. In this latter case the solar module is inherently safe and the hot spot is not a concern.

196 **III. Circuit realization and costs**

197

198 The complete bypass circuit, including all details about its continuous biasing, are reported in Fig.4
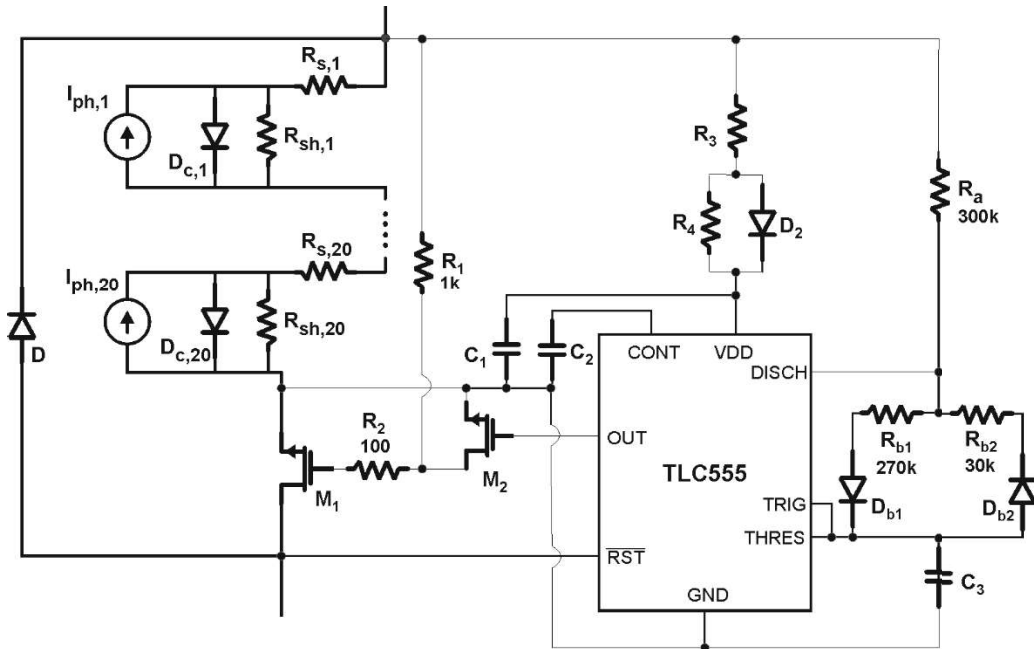
199

200 Fig. 4. Detailed circuit schematic of the proposed bypass solution.

201

202 As can be inferred, the figure is similar to Fig. 3, with the difference that the solar cells are described by

203 means of the one diode model (d'Alessandro et al., 2015);the TLC555 is shown along with its polarization

204 network, realized according with the guidelines reported in (Texas Instruments, 2016).In particular, the

205 group formed by R_3, R_4, C_1, and D_2, supplies the operating voltage to the integrated circuit. The capacitor

206 C_1, which is connected from V_{DD} and ground (GND), stabilizes the supply voltage. At the start it is rapidly

207 charged through R_3 and D_2. If the voltage supplied by the solar panel decreases, the discharge of C_1 occurs

208 through the series R_4-R_3, so that, choosing an high value for R_4 (the values of all components are reported

209 in Table 1), guarantees slow discharge. It must be remarked that the TLC555 correctly operate with

210 polarization voltages between 2 V and 15 V, this fact means that the solar panel can supply the circuit in

211 all illumination conditions of practical interest. It is also important to point out that the circuit only leaks

212 360 µA for its continuous operation, with a power consumption of few mW.

213 The group formed by R_a, R_{b1}, R_{b2}, D_{b1}, D_{b2}, and C_3, allows setting the frequency of the oscillator and the

214 duty cycle. Formulas for setting these parameters can be found in (Rogers, 2002). By summarizing we can

8

215 say that the resistances control the charging and discharging time constants of C_3, whose oscillating
216 voltage triggers oscillation period T, was chosen to have T=0.63 s, while R_{b2}, related to the duty cycle,
217 was realized by means of a potentiometer allowing to vary the duty cycle in the range 2% - 50%.
218 R_1 is chosen to limit the current through M_2 (when M_2 is conducting) to few mA while R_2 is chose to slow
219 down the switching time of M_1. C_2 stabilizes the threshold for the triggering of the oscillations.
220 A photograph of the resulting prototype is shown in Fig. 5.
221

222
223 Fig. 5. Rear side photovoltaic module junction box containing
224 three bypass circuits. In the periphery the board contains
225 additional circuits for sensing purposes.
226

227 The I-V curve of the solar panel equipped with this prototype (see also Section V) are compared in Fig. 6
228 with the I-V curve of the same solar panel equipped with the standard bypass diode.
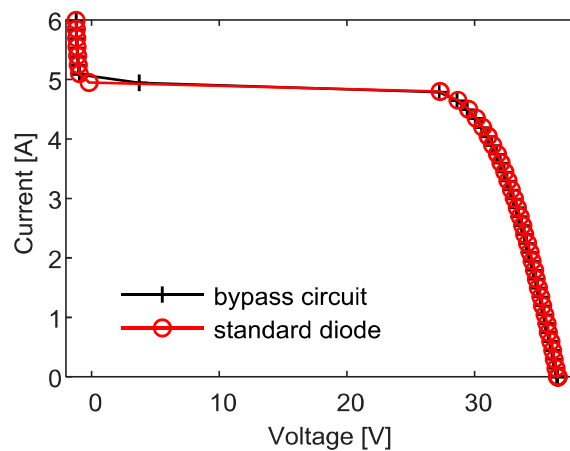
229
230 Fig. 6.   I-V curves comparison: a 60-cells poly-Si module
231 equipped with standard diodes (red line) is compared to the
232 one adopting the proposed solution (black line).

9

233

234 As can be seen the two curves are almost identical; this means that the bypass circuit does not introduce

235 any disturbance when the solar panel is connected in a series string.

236 Some details about the cost of the circuit are reported in Table I. The extra cost with respect to the

237 standard bypass diode is about 2 €.

238

TABLE I

Part Name	Description	Unit Price [€]
TLC555	Astable Circuit	0.33[1]
M_1	N-channel MOFET 40V 100A	0.78[1]
M_2	N-channel MOFET 30V 2.6 A	0.21[1]
D	Schottky diode 50V 20A	0.42[1]
Biasing devices	SMD resistors ¼ W, Diodes, Ceramic capacitors	0.34
PCB	Production and Components Soldering	0.5
	Total cost	2.58

239 [1]online catalogue for a quantity of 1000 units.
240

241 The incidence of this cost depends on the number of solar cells forming the solar panel. Usually, one

242 bypass device protects about 20 solar cells so that the extra cost is about 0.1 € per solar cell. The incidence

243 of the cost in relation to the producible energy can be evaluated by assuming an expected lifetime for the

244 solar panel of 25 years and a average producible energy of 1300 kWh/kWp/year; for a 5 Wp solar cell this

245 means an extra cost of about 0.0001 €/ kWh. By considering that the cost of a solar cell is about 0.5 €/Wp,

246 the weight of the extra cost per kWh is about 1%.

247 Another concern for the bypass circuit is reliability. It is quite obvious that adding electronic devices

248 introduces reliability issues; however, in this case, the goal is to bring such issues outside the solar panel,

249 whose value is greater by orders of magnitude. Moreover, it should be considered that adopted power

250 devices are automotive devices rated to handle high currents (100 A) at high switching frequencies

251 (hundred of kHz) with an expected lifetime of several years. The proposed application is for much lower

252 currents and almost stationary operation, so that the expected lifetime becomes much longer than the

253 normal life cycle of the solar panel itself.

254

255 **IV. Circuit simulation**
256

257 Simulations were carried out by analyzing the circuit shown in Fig.4. This circuit represents a sub-module

258 made by 20 solar cells; simulations were carried out by connecting in series three of these circuits, thus

259 simulating the behavior of a photovoltaic module made by three sub-modules, hereinafter referred to as

260 #1, #2, and #3. In order to compare the proposed solution with the standard bypass approach, the

10

261 MOSFET M_1 belonging to sub-module #1 was short circuited, thus reducing the circuit to that of Fig. 1a.

262 A tracking algorithm, driving the operating point toward the maximum power point (MPP), was also

263 embedded in the simulations.

264 Simulated experiments were conducted by creating a current mismatch in sub-module #1 and sub-module

265 #3 with respect to sub-module #2, so that the corresponding bypass devices turned ON. The mismatch was

266 caused by assigning a reduced photogenerated current (current sources $I_{ph,i}$ in Fig. 4) to only one solar cell

267 per sub-module, so as to emulate the partial shadowing of sub-modules #1 and #3. As mentioned in the

268 previous section such a situation leads to the reverse biasing of the shaded cells.

269 The current mismatch was chosen small enough to reproduce the worst conditions in terms of the power

270 dissipated over the shaded cells, as defined by the EN 61215 and corresponding to a small shadow

271 covering the cells. This situation has been also experimentally reproduced, as described in the next

272 section.

273 The irradiance profile which is supposed to illuminate the solar cells is shown in Fig. 7.

274 As can be seen, sunny cells are supposed to be subject to a constant irradiance of 1000 W/m^2 (i.e., 1 Sun),

275 thus supplying their nominal current. In order to test the capability of the new bypass circuit to recognize

276 the occurrence of the shadow, and to recover normal operation when this condition ceases, shaded cells

277 were subject to a varying irradiance, passing from 1000 W/m^2 to 930 W/m^2 and vice-versa.

278 Let's start by analyzing the voltages across each sub-module, shown in Fig. 8.

279
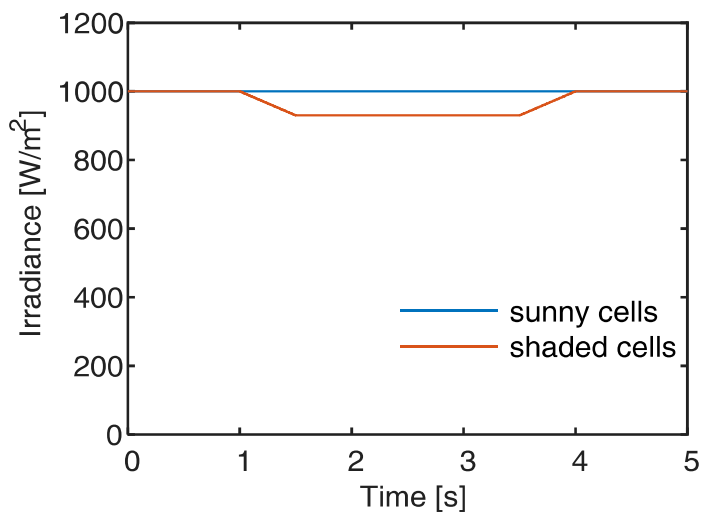
280 Fig. 7. Simulated irradiance profile adopted to emulate a
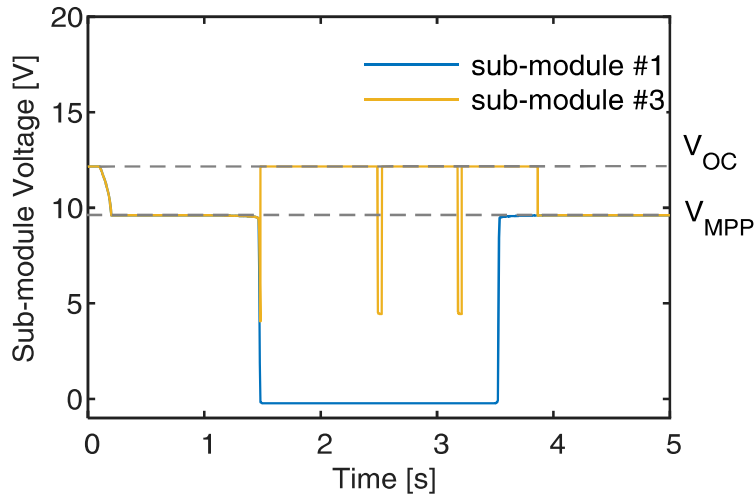281 current mismatch in the photovoltaic module.
282

11

Fig. 8.   Voltages supplied by the sub-modules during time varying irradiance conditions depicted in Fig.6.

As starting condition, t=0, the sub-modules were assumed open circuited, as a consequence, the voltage at their terminals was the open circuit voltage V_{oc}. Subsequently, the MPP Tracking (MPPT) algorithm found the MPP and the voltage decreased to V_{MPP}. At t=1s (see Fig. 7) the irradiance over shaded cells started to decrease and, at about t=1.5s, the current mismatch was large enough to trigger the turn ON of the protection devices. It is important to note that both protection systems turn ON simultaneously, thus evidencing that no delays are introduced by the new circuit. On the other hand, the behavior of the two sub-modules is totally different. In fact, while the voltage across sub-module #1 was small and negative (equal to the voltage drop across the forward biased bypass diode), the voltage across sub-module #3 reached V_{OC}, thus demonstrating that the series MOSFET interrupted the current. As can be seen, the voltage across sub-module #3 decreased periodically, this fact is due to the action of the oscillator that checks the persistence of the bypass conditions, as long as a current mismatch exists the voltage returns to V_{OC}; conversely, when the mismatch ceases, sub-module #1 promptly recovers V_{MPP}, while sub-module #3 waits for the change of state of the oscillator, after that, V_{MPP} is recovered as well. Therefore, the maximum time allowed for the temperature of the shaded cell to increase is equal to the period of the oscillator.

The effect of the bypass circuits on the shaded cells is better evidenced in Fig. 9.
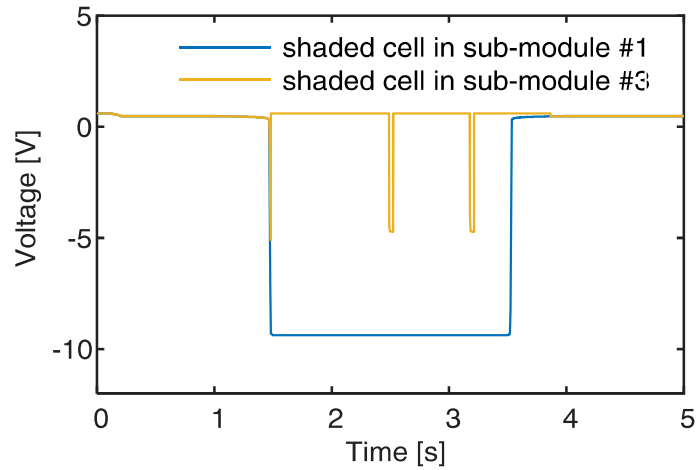
12

Fig. 9. Voltages across shaded solar cells in sub-modules protected by a standard bypass diode (blue curve) and by the proposed bypass circuit (yellow curve).

As can be seen, during the mismatch, the shaded cell in sub-module #1 was strongly reverse biased (thus heating up), while the shaded cell in sub-module #3 was open circuited for the most part of the time. It is interesting to note that the reverse voltage across the shaded cell in sub-module #3 remains lower than the other also during the shadow checks; this fact depends on the presence of the series MOSFET which shares part of the total voltage, as illustrated in Fig. 1.

Finally, Fig. 10a shows the drain to source voltages, V_{DS}, across the MOSFETs M_1 and M_2 of the bypass circuit, that, according to Fig. 3 coincide, respectively, with the supply voltage of the oscillator and with the driving voltage, V_{GS1}, of M_1; while, Fig. 10b reports the output voltage of the oscillator, that coincides the driving voltage of M_2.
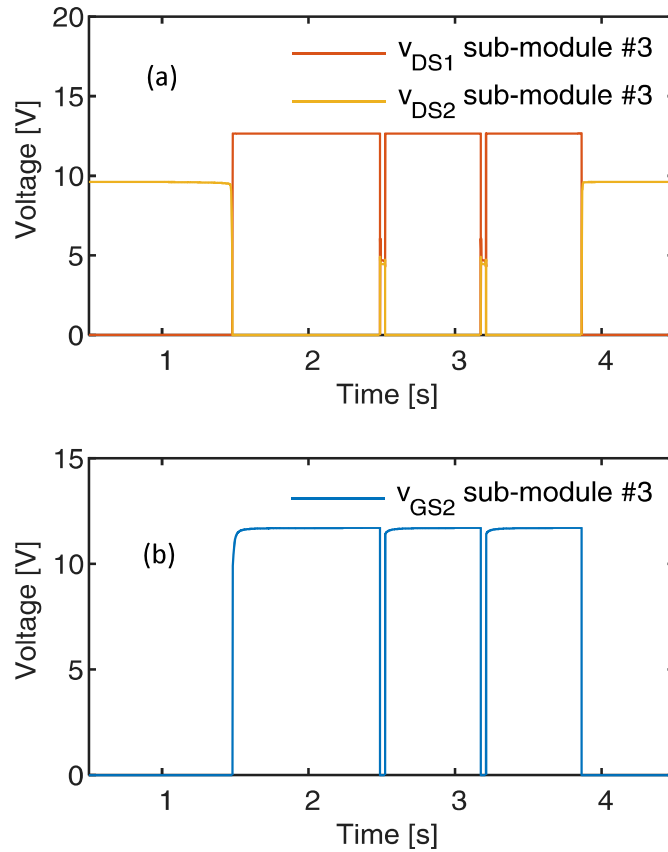
Fig. 10. Driving voltages of the active devices forming the proposed bypass circuit.

During normal operation (no current mismatch), the driving voltage for M_1 (V_{DS2}) is high (equal to V_{MPP}) and V_{DS1} is near zero; when the mismatch occurs (t=1.5s), the oscillator is switched ON and its output signal (V_{GS2} in Fig. 10b) starts to oscillate. When V_{GS2} is high, M_2 is turned ON, as evidenced by V_{DS2} in Fig. 9a that decreases to near zero, consequently M_1 is switched OFF. When V_{GS2} is low (mismatch check) M_1 turns ON, but, if the mismatch is still present, V_{DS1} remains high enough to power supply the oscillator, so that M_1 turns OFF again when V_{GS2} recovers the high value. On the contrary, when the attempt to turn ON M_1 (V_{GS2} low) occurs in absence of current mismatch, V_{DS1} decreases to near zero, so that the oscillator is switched OFF and the normal operation is recovered.

V. Experiments

In order to experimentally verify the performance of the new bypass circuit an electronic board (shown in Fig.5), suitable to be hosted in the standard junction box mounted in the rear side of photovoltaic modules, was designed and fabricated.

14

335   The photovoltaic module adopted for the experiments is shown in Fig. 11; it was made by 60 solar cells,

336   grouped in three sub-modules (hereinafter referred to as #1, #2, and #3 as for the simulations), the board

337   contained three separate bypass circuits. In order to test the new circuit in comparison with the standard

338   bypass diode the MOSFET M_1 of the bypass circuit of sub-module #1 was short circuited as in the

339   simulations. Two kinds of experiments were carried out, in the first case a dynamic shadow, advancing

340   and regressing over a solar cell embedded in sub-module #3 was considered. In such a case, the capability

341   of the bypass circuit to recognize the mismatch and to recover the normal operation, was tested. This

342   experiment can be directly compared with the simulations. In the second case, in order to test the

343   capability of the circuit to prevent the hot spot, two solar cells, belonging, respectively, to sub-module #1

344   and sub-module #3, were partially obscured.

345

346

347   Fig. 11.   The 60-cells module adopted for experiments.
348   Second case test set-up: partially shaded solar cells belonging
349   to different sub-modules. The cell on the left is protected by
350   the standard bypass diode, the cell on the right by the new
351   bypass circuit.

352

353   In the first case significant electrical parameters were monitored. A photograph of the signals acquired by

354   a digital oscilloscope is shown in Fig. 12.

Fig. 12. Digital oscilloscope view of electrical signals during a bypass event.

The yellow and the blue curves are, respectively, the string current and the current in sub-module #3.The purple and the green curves are, respectively, the drain to source voltage of M_1 and the gate to source voltage of M_1.

To make the interpretation easier, signals are shown separately in the following figures. From these figures it can be derived that the period of the oscillator was set to about 0.6s with duty cycle 96.5%; hence, the duration of the mismatch check was about 21ms.

As can be inferred from Fig. 13a, sub-module #3 was shadowed at about -1.5 s.

The correct intervention of the bypass circuit is witnessed by the interruption of the sub-module current, as well as by V_{DS1}, reported in Fig. 13b, that reached the open circuit voltage. Moreover, the figure shows that the driving voltage of M_1, V_{GS1}, periodically tried to turn ON M_1, but, since shadow was not yet removed, the open circuit condition was promptly recovered when V_{GS1} returned low.

The return to normal operation, when the shadow was removed, is shown in Fig. 14(note that a new timescale is adopted because the figure comes from a new acquisition).

In this case, in the interval of time between 0.5 s and 1s the shadow was removed, so that, after the first time V_{GS1} was made high, at about 1s, M_1 turned ON (V_{DS1} went to zero) and the sub-module supplied again the normal operating current.

The definitive evidence of the correct behavior of the bypass circuit is given by the thermal analysis. The experiment was carried out by applying an opaque shield on two solar cells, as shown in the photograph reported in Fig. 11.
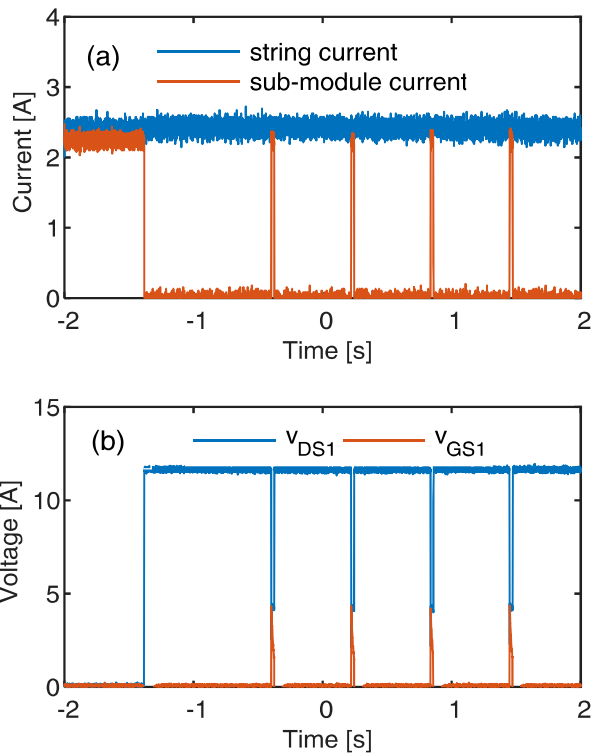
378

379   Fig. 13. (a) Currents and (b) voltages measured at the onset of the bypass event.
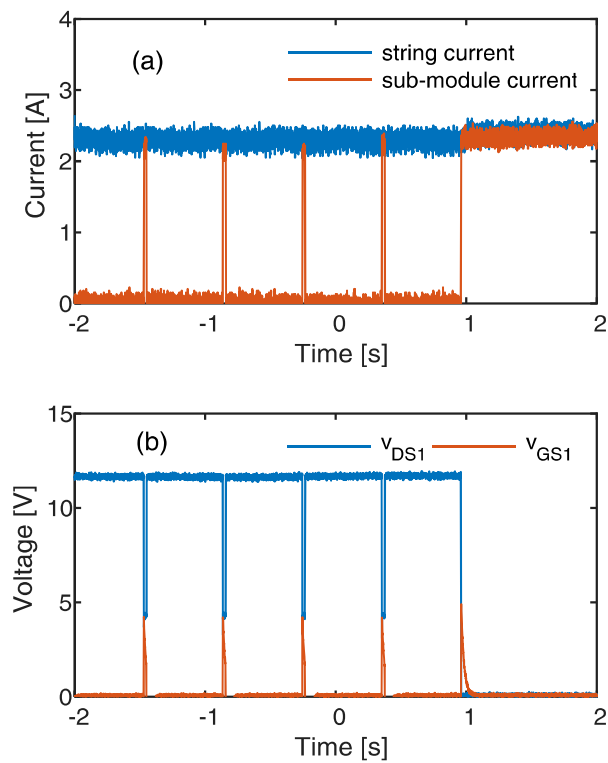
380

381

382   Fig. 14. (a) Currents and (b) voltages measured at the end of the bypass event.

17

383 The area of the shields was chosen by following the procedure for the "Hot spot endurance test" described

384 in the EN 61215 to cause the maximum expected power dissipation over the solar cells. The shaded cell

385 in the left side belonged to sub-module #1, hence it was protected by the standard bypass diode only; the

386 shaded cell in the right side belonged to sub-module #3, hence it was protected by the modified bypass

387 circuit. During this experiment the irradiance was about 800 W/m^2, corresponding to a photogenerated

388 current supplied by the sunny cells of about 6.7 A.

389

390 Current and voltages corresponding to such conditions are reported in Fig. 15.

391 In particular, in Fig. 15a the current supplied by the sunny cells, indicated as "string current", is compared

392 to the currents flowing through the shaded cells. As can be seen, the current flowing through the cell not

393 protected by the bypass circuit is about 5.85 A, coinciding with the current at the maximum power point

394 MPP (according to the operating conditions prescribed by the EN 61215). The current flowing through the

395 cell protected by the bypass circuit is zero, thanks to the opening of the series MOSFET. At the same time,

396 as shown in Fig. 15b, the voltage across the sub-module with the bypass circuit was about 11 V, which is

397 the open circuit voltage (since no current is flowing), while the voltage across the sub-module without the

398 bypass circuit is -0.43 V (because of the intervention of the standard bypass diode). Consequently, the

399 power dissipated by the sub-module equipped with the bypass circuit (Fig. 15c) was zero, while the sub-

400 module not protected by the bypass circuit was dissipating an overall power P of about 2.5 W.

401 In this regard it is worth noting that, actually, only the shaded solar cell was dissipating power, while the

402 others were working at the MPP. Therefore, the power dissipated by the shaded solar cell can be evaluated

403 by considering that the overall power P produced by the sub-module is given by

404
$$P = \sum_{i=1}^{20} V_i \cdot I_{string} = 19 \cdot V_{MPP} \cdot I_{string} + V_{Shad} \cdot I_{string} \qquad (3)$$

405 where V$_{shad}$ is the voltage across the shaded cell. This equation leads to

406
$$V_{Shad} \cdot I_{string} = P - 19 \cdot V_{MPP} \cdot I_{string} = -55.8W \qquad (4)$$

407 In contrast, the shaded cell protected by the bypass circuit dissipated zero power.

408 Above results justify the thermal image shown in Fig. 16, taken by means of an IR camera FLUKE TiS56.

409 As can be seen, the solar cell on the left side, not protected by the bypass circuit, got extremely hot, while

410 the solar cell protected by the bypass circuit was cold (the position of the shield can be individuated as a

411 colder area in the white circle). It is interesting to note that the right side of the photovoltaic module (that

412 coincides with sub-module #3) showed an average temperature higher than the left side, this is a further

413 evidence that sub-module #3 operated in open circuit conditions (it is worth remembering that open

414 circuited solar cells do not convert Sun power into electrical power, hence, the operating temperature gets

415 higher). The hot shape on the left, off the photovoltaic module, is the load adopted to fix the operating
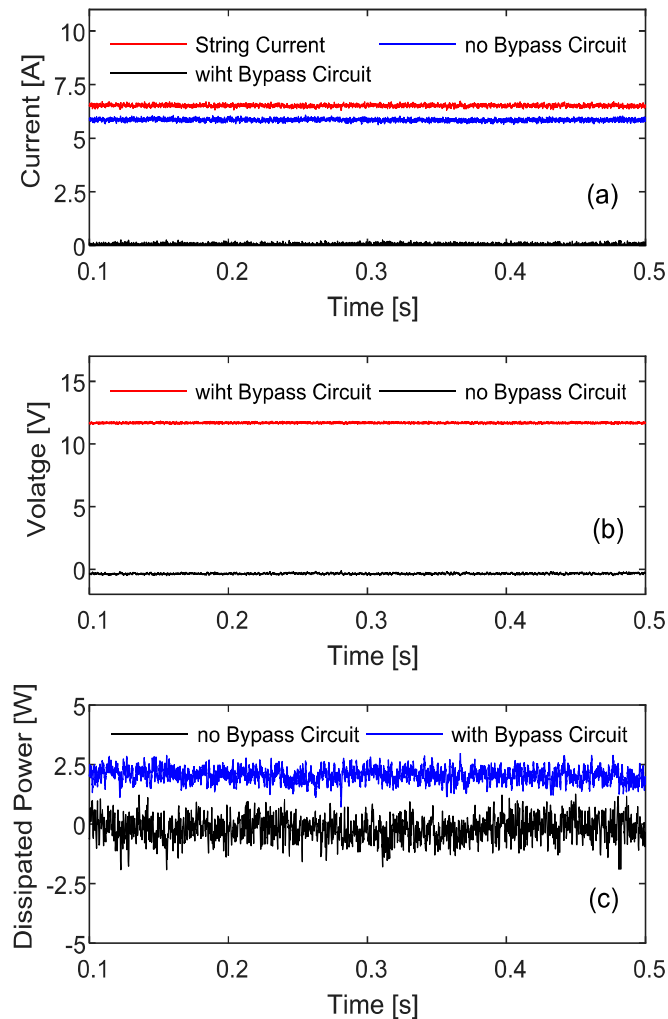
416   point.

Fig. 15.   Currents (a), and voltages (b) corresponding to the shading conditions of Fig. 11. Power dissipation (c) with and without the bypass circuit.

422   From this figure the temperature profile along a cutting line passing through the center of the two shaded

423   cells has been extracted. This profile, reported in Fig. 17, shows that the hot cell reached a temperature of

424   about 103°C, with a temperature increment of about 50°C with respect to normal operating cells.

425   Conversely, the shaded cell, belonging to sub-module #3 and protected by the new bypass circuit,

426   remained at the normal operating temperature, with an expected small increment on the exposed surface

427   depending on the open-circuit operation.
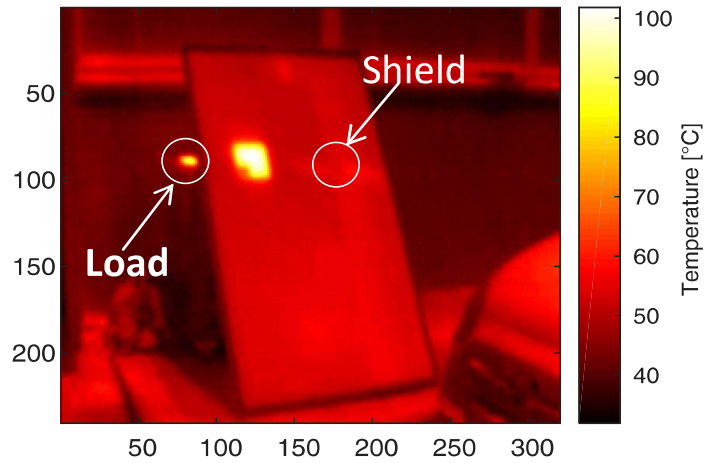
Fig. 16.Thermal image of the partially shaded photovoltaic module shown in Fig.13.
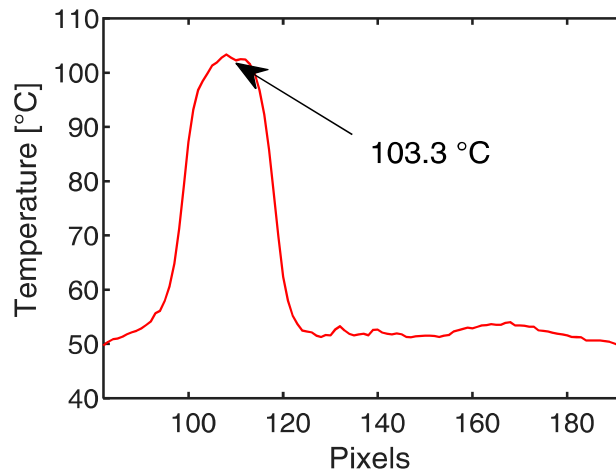
Fig. 17. Thermal profile along a cutting line passing through the center of the shaded solar cells.

VI. Conclusions

In this paper a new bypass circuit has been presented. The circuit prevents the formation of hot spots in malfunctioning solar cells by interrupting the current circulating in the corresponding sub-module, thus inhibiting power dissipation. With respect to other solutions based on the same principle, the proposed circuit has an "analogical" behavior, in the sense that it is self-activating when mismatch conditions occur, without needing micro-processors or other complex logic circuits. Simulations and experiments have evidenced that the hot spot can be effectively prevented. In the worst case operating conditions, as defined by the EN 61215, a difference of about50 °C, has been found between a shaded solar cell protected by a

20

445 standard bypass diode and, in the same operating conditions, a solar cell protected by the new bypass

446 circuit.

447

448 **References**

449 AN3432 ST Application note [WWW Document], 2011. https://doi.org/019041 Rev 1

450 Bressan, M., Gutierrez, A., Garcia Gutierrez, L., Alonso, C., 2018. Development of a real-time hot-spot
451   prevention using an emulator of partially shaded PV systems. Renew. Energy 127, 334–343.
452   https://doi.org/10.1016/j.renene.2018.04.045

453 d'Alessandro, V., Di Napoli, F., Guerriero, P., Daliento, S., 2015. An automated high-granularity tool for
454   a fast evaluation of the yield of PV plants accounting for shading effects. Renew. Energy 83, 294–
455   304.

456 d'Alessandro, V., Guerriero, P., Daliento, S., 2014. A simple bipolar transistor-based bypass approach for
457   photovoltaic modules. IEEE J. Photovoltaics 4, 505–513.

458 Daliento, S., Di Napoli, F., Guerriero, P., d'Alessandro, V., 2016. A modified bypass circuit for improved
459   hot spot reliability of solar panels subject to partial shading. Sol. Energy 134.
460   https://doi.org/10.1016/j.solener.2016.05.001

461 Dhimish, M., Holmes, V., Mather, P., Sibley, M., 2018. Novel hot spot mitigation technique to enhance
462   photovoltaic solar panels output power performance. Sol. Energy Mater. Sol. Cells 179, 72–79.
463   https://doi.org/10.1016/j.solmat.2018.02.019

464 García, M., Marroyo, L., Lorenzo, E., Marcos, J., Pérez, M., 2013. Observed degradation in photovoltaic
465   plants affected by hot-spots. Prog. Photovoltaics Res. Appl. 24, 1292–1301.
466   https://doi.org/10.1002/pip.2393

467 Ghanbari, T., 2017. Hot spot detection and prevention using a simple method in photovoltaic panels. IET
468   Gener. Transm. Distrib. 11, 883–890. https://doi.org/10.1049/iet-gtd.2016.0794

469 Green, M.A., 1986. Solar cells : operating principles, technology and system applications. University of
470   New South Wales., Kensington.

471 Jordan, D.C., Kurtz, S.R., 2013. Photovoltaic Degradation Rates-an Analytical Review. Prog.
472   Photovoltaics Res. Appl. 21, 12–29. https://doi.org/10.1002/pip.1182

473 Kaplani, E., 2012. Detection of degradation effects in field-aged c-Si solar cells through IR thermography
474   and digital image processing. Int. J. Photoenergy 2012. https://doi.org/10.1155/2012/396792

475 Kim, K.A., Krein, P.T., 2015. Reexamination of Photovoltaic Hot Spotting to Show Inadequacy of the
476   Bypass Diode. IEEE J. Photovoltaics 5, 1435–1441.
477   https://doi.org/10.1109/JPHOTOV.2015.2444091

478 Kim, K.A., Krein, P.T., Seo, G.S., Cho, B.H., 2013. Photovoltaic AC parameter characterization for
479   dynamic partial shading and hot spot detection. Conf. Proc. - IEEE Appl. Power Electron. Conf.
480   Expo. - APEC 2, 109–115. https://doi.org/10.1109/APEC.2013.6520194

481 Niazi, K., Khan, H.A., Amir, F., 2018. Hot-spot reduction and shade loss minimization in crystalline-
482   silicon solar panels. J. Renew. Sustain. Energy 10, 033506. https://doi.org/10.1063/1.5020203

483 Olalla, C., Hasan, M., Deline, C., Maksimović, D., 2018. Mitigation of Hot-Spots in Photovoltaic Systems

484   Using Distributed Power Electronics. Energies 11, 726. https://doi.org/10.3390/en11040726

485   Philipps, S., Warmuth, W., 2018. PHOTOVOLTAICS REPORT [WWW Document].

486   Rogers, P., 2002. Design low-duty-cycle timer circuits [WWW Document]. Bill Travis. URL
487   www.edn.com

488   Sanchez-Friera, P., Piliougine, M., Pelaez, J., Carretero, J., Cardona, M.S. de, 2011. Analysis of
489   degradation mechanisms of crystalline silicon PV modules after 12 years of operation in Southern
490   Europe. Prog. PHOTOVOLTAICS Res. Appl. 19, 658–666. https://doi.org/10.1002/pip.1083

491   Spanoche, S.A., Stewart, J.D., Hawley, S.L., Opris, I.E., 2013. Model-Based Method for Partially Shaded
492   PV Module Hot-Spot Suppression. IEEE J. Photovoltaics 3, 785–790.
493   https://doi.org/10.1109/JPHOTOV.2012.2230054

494   Texas Instruments, 2016. TLC555 LinCMOS Timer [WWW Document]. URL
495   http://www.ti.com/lit/ds/symlink/tlc555.pdf

496